Linking dynamics and structure in highly asymmetric ionic liquids

Juan C. Avilés-Sánchez,[1,*] Ernesto C. Cortés-Morales,[2,†] Mariana E. Farías-Anguiano,[3,1,‡] Jonathan K. Whitmer,[2,4,§] and Pedro E. Ramírez-González[5,¶]

[1] *Instituto de Física "Manuel Sandoval Vallarta", Universidad Autónoma de San Luis Potosí, Álvaro Obregón 64, 78000 San Luis Potosí, SLP, México.*

[2] *Department of Chemical and Biomolecular Engineering, University of Notre Dame, Notre Dame, IN 46556, USA.*

[3] *División de Ciencias e Ingenierías, Universidad de Guanajuato, Loma del Bosque 103, 37150 León, Gto., México*

[4] *Department of Chemistry and Biochemistry, University of Notre Dame, Notre Dame, IN 46556, USA.*

[5] *CONAHCyT IxM-Instituto de Física "Manuel Sandoval Vallarta", Universidad Autónoma de San Luis Potosí, Álvaro Obregón 64, 78000 San Luis Potosí, SLP, México.*

(Dated: July 9, 2025)

Abstract

We explore an idealized theoretical model for the ion transport within highly asymmetric ionic liquid mixtures. A primitive model (PM)-inspired system serves as a representative for asymmetric ionic materials (such as liquid crystalline salts) which quench to form disordered, partially-arrested phases. Self-Consistent Generalized Langevin Equation (SCGLE) Theory is applied to understand the connection between the size ratio of charge-matched salts and their average mobility. Within this model, we identify novel glassy states where one of the two charged species (without loss of generality, either the macro-cation or the micro-anion) are arrested, while the other retains liquid-like mobility. We discuss how this result is useful in the development of novel single-ion conducting phases in ionic-liquid-based materials. For instance, the developing of conductors operating at low-temperature or the technology associated with ionic liquid crystals.

* email: jcaviles@ifisica.uaslp.mx

† email: ecortesm@nd.edu

‡ email: mfariasa@ifisica.uaslp.mx

§ email: jwhitme1@nd.edu

¶ email: pramirez@ifisica.uaslp.mx

I. INTRODUCTION

The design of structurally stable, high-conductivity electrolytes is a key materials challenge for modern energy storage, with wide-ranging implications for the future of battery technologies. Ionic liquids (ILs) and their close relatives—polymerized ionic liquids (PILs), room temperature molten salts (RTMS) and deep eutectic solvents (DES)—have been of particular interest, comprising a class of materials attractive for favorable material properties [1, 2], including a wide temperature range over which the materials are chemically stable, in the liquid phase, and maintain high ionic conductivity [2, 3]. In addition to applications in energy storage[4], ionic liquids have been promising as catalysts [5, 6], plasticizers[7] and in desalination membranes [8].

Many common ILs are formed by combining a larger cation, often affixed with alkyl chains of varying length, with a smaller organic or inorganic anion [9]. Many methods have been explored to discern IL structural properties, both theoretically and in simulation. For the later, it is common practice to implement Molecular Dynamics and Monte Carlo simulations[10] which allow for connections between molecular structure and thermodynamic or dynamical properties. Many developments have been achieved in IL simulations, and for this work we will refer to the specialized studies[11] into the phase transition of IL crystals[12]. Even with specialized and accurate simulations for the prediction of material properties in a chemical complex of interest, general trends can be missed by such specific models. Hence the need to develop model representations and theoretical tools that aid in guiding the design and study of new IL materials. Though much of the discussion regarding solid ionic liquids focuses on the crystalline phase, ILs can readily form arrested glasses [13–26], and exploration of these amorphous glassy states presents an opportunity to more deeply understand links between molecular structure and dynamics in these materials. Historically, other scientific communities (such as metallurgists) have found great advantage in the application of amorphous materials.[27, 28] Thus, the study of amorphous solid conductors could be a new branch of development within the conductors community. For example, batteries working at low-temperatures cloud be designed using partially-arrested states since glass transition usually presents at such conditions. Regarding asymmetric ionic liquids, the prediction of amorphous solid states represents applications of such systems in condensed states which have not been envisioned by other groups. Most of the ionic liquids applications were proposed

as substitutes of conventional solvents, i.e., in liquid state. Exploring other phases or states extends the opportunity for developing novel applications for ionic liquids.

In this paper we describe a very simple theoretical model adequate for initial description of amorphous states of ILs. Our main objective is the description of partially-arrested states, in which one of the ions is in a glassy state and the other one presents a fluid-like behavior. Such a model is based on the naive assumption of spherical form for the ions, which allows the possibility of applying a simple model for the structural properties. In order to test the predictive power of the theoretical model, we performed all-atom molecular dynamics simulations of imidazolium-based ILs. Surprisingly, such a simple approach describes the overall scenario of the glassy dynamics of highly-asymmetric ILs, showing that our naive model could be a great first approach in the understanding of glassy behavior in complex ILs. The work is organized as follows, section II presents the computational details of the MD simulations. Section III describes the main elements of our simple theoretical model for ILs. Section IV show quantitative comparison between theory and MD simulations and finally section V discuss the main conclusions of our work.

II. COMPUTATIONAL DETAILS AND SIMULATION METHODS

In order to compare the theoretical predictions we performed a series of all-atom simulations of imidazolium-based ionic liquids (see Fig. 1). All our simulations were performed using Gromacs 2022.2 MD simulation package [29, 30]. cubic boxes of 8 nm on each side were generated, where 1024 ion pairs were inserted randomly avoiding overlapping. AMBER94 [31] force field was used to define the atomic interactions. All the force field parameters were taken from reference [32]. As usual, all-atom MD simulations are limited by the strength of the chosen force field. However, AMBER94 force field have been used in the past for studying glassy behavior in the context of ionic liquids [33]. In any case, the possibility of improving the force field is always open.

Periodic boundary conditions (PBC) were applied to all three dimensions of a cubic simulation box, and a 1.6 nm cutoff was set to the non-bonded interactions. The long-range electrostatic interactions [34, 35] were handled with the particle mesh Ewald (PME) method [36]. The two systems contain 1024 ion pairs. In our study, we chose $T = 500K$ as one of the target simulation temperatures since the experiment has demonstrated that this

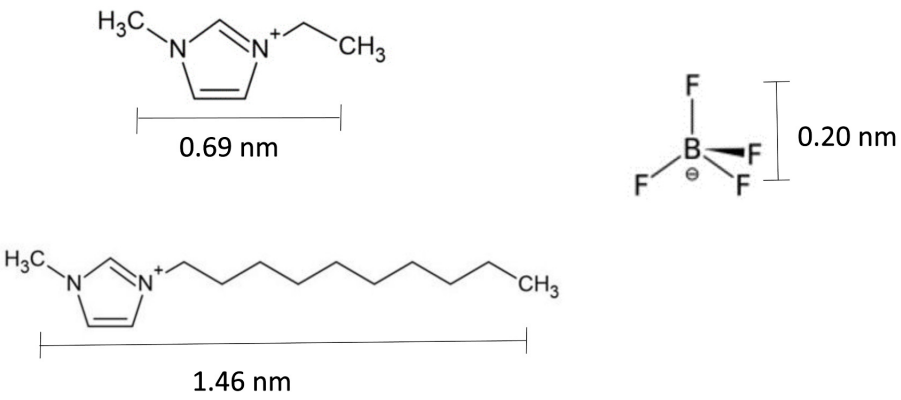

FIG. 1. The systems analyzed are binary mixtures of charged components, where a size asymmetry is present in the system. Theoretical models of charged hard spheres were developed based on the $[C_nMim]^+[BF_4]^-$ ionic liquids with $n = 2$ and 10 (shown in the figure). Hence, size asymmetries have been chosen from the size ratio among cation and anion in each case

.

temperature is well above the melting temperature of $EMI^+BF_4^-$ [37].

The initial random configuration went through a series of NPT simulations at a constant pressure $P = 100\ atm$ and different temperatures from $T = 2000K$ down to 1500, 1000, 800, 600, and $500K$. At each temperature, the system was simulated for 1 ns. The last configuration was then equilibrated with a 1 ns NPT simulation at $P = 1atm$ and $T = 500K$ to obtain the average simulation volume V. After that, the system further went through another simulated annealing procedure in the NVT ensemble with the same temperature sequence and the determined V.

In order to analyze homogeneous systems we performed NPT production runs. The equilibrated configuration went through the production runs in the NPT ensemble at $T = 500K$. For production runs the systems were simulated during 10 ns. In order to explore lower temperatures, we perform a NPT annealing from $500K$ to the target temperature for 1 ns. Then a NPT production run where performed at each target temperature to calculate the structural and dynamical properties. Cations with longer chains required 100 ns-runs in order to obtain reliable results for dynamical properties.

III. THEORETICAL MODEL AND METHODS.

The basis for past analytical studies of ionic liquid properties is the closure to the Ornstein–Zernike[38] equation formulated by Waisman and Lebowitz, known as the MSA (mean spherical approximation)[39, 40]. Here we explore a simplified representation of ILs based on the primitive model (PM)[41] solution of the MSA with dynamical behavior determined through a generalized Langevin equation representation. We will return to this formulation in detail later, for now it is sufficient to mention that this is not the only theoretical approximation for the study of electrolytes and IL, there are plenty of theoretical approximations such as: the widely used Debye-Hückel limiting laws[42], the Generalized MSA[43], or the Binding MSA[44], among several others.

The theoretical framework known as Self-Consistent Generalized Langevin Equation (SCGLE) theory has been previously applied to a wide variety of systems, both purely theoretical and realistic model substances. It has been able to successfully predict thermodynamic[45] and dynamical properties, in particular: dynamical arrest diagrams, MSD and diffusion coefficients of complex chemical compounds such as room temperature molten salts,[33] and low-density colloidal Wigner glasses.[46, 47] In the present work, we employ the SCGLE framework, developed specifically for ionic liquids by Farias-Angiano *et. al.* [48], to determine the arrest diagram and MSD of a theoretical system composed of a charged hard sphere binary mixture with size asymmetry between the cation and anion.

Without loss of generality, we will refer to the larger species (macro-ion) as the cation and the smaller species (micro-ion) as the anion, as depicted in Fig.1. Though similar models have been explored before using the SCGLE, the ionic mobility in the mixture and its effect on conductivity has not been fully explored yet, which is our primary interest here. The use of size asymmetry, even without charge symmetry, results in domains within the temperature-concentration plane which yield arrest of the cation, anion, or both. The partially-arrested states, where one of the ionic components remains fluid, arise in this system due to the size asymmetry, and allow us to map out a phase space relevant for single-ion conducting electrolytes.[49, 50] While our model is a coarse approximation of the molecular structures present in real ionic liquids and their derivatives, this work provides a crucial first step towards a detailed theoretical modeling of ionic liquids, and toward engineering materials with optimal conductivity and stability across a wide range of temperatures. Such a model

surely is limited due to the non-spherical shape of the ionic liquids studied and, as well, by the MSA solution for structural inputs. The improvement of structural inputs beyond MSA is work in progress which requires additional effort. Regarding the non-spherical shape, there exists an extension of the SCGLE theory for non-spherical systems [51], which has been applied to the calculation of dynamic arrest lines for spherical particles interacting by a dipolar (magnetic-like) potential [52]. Such an extension of the theory could be applied to molecules with non-spherical shapes. Unfortunately, a robust method for numerical solutions in such cases has been elusive until now. We expect to overcome such barriers soon.

IV. QUANTITATIVE COMPARISONS BETWEEN SIMULATION AND THEORY.

An illustration of the coarse-grained model we utilize as well as a typical configuration of systems shown in Fig. 1. The sizes of the cations and anions is roughly determined by the average distance between the hydrogens attached to the CH_3 group at both extremes of the cations. Regarding the anions, we take the average diameter as the double of the distance between boron and one fluorine. Average diameters are also shown in Fig. 1. Note that we specifically choose alkyl tail lengths with $n = 2$ and 10 in the homologous C_nMIm series to avoid liquid-crystal forming molecules [14].

In the resulting model, we define parameters for the cation using the subscript p reflecting its positive charge, while the anion parameters are labeled by a subscript m referring to their negative (minus) charge. Both species are modeled as charged hard spheres. The diameter of the larger cation species is chosen as the unit of length to normalize our calculations, $\sigma_{\rm p} = 1.0$. The anion diameter $\sigma_{\rm m}$ is chosen according to the size ratio between cations and anions. Both species have an equal and opposite charge $|z_i| = e$, and the total number of ions is such that the system complies with the global electro-neutrality condition required in the MSA closure $\sum_i \rho_i z_i = 0$. The size asymmetry in these systems is captured by the dimensionless quantity $\xi = \sigma_p/\sigma_m$, which has been previously shown to be within the limits of validity for the SCGLE framework.[48, 53]

For simplicity in our calculations, we will employ the Hiroike solution[54] to the MSA

previously mentioned and proposed by Blum[55] within the PM:

$$\begin{aligned} h_{ij}(r) &= -1 \qquad \text{for } r \leq \sigma_{ij} \\ c_{ij}(r) &= -\beta \frac{e^2 q_i q_j}{\varepsilon_0 r} \quad \text{for } r > \sigma_{ij} \end{aligned} \tag{1}$$

for the direct correlation function of the ion pair $c_{ij}(r)$ and the total correlation function $h_{ij}(r)$, with $\sigma_{ij} = (\sigma_i + \sigma_j)/2$ the arithmetic mean of ionic diameters σ_i and σ_j. These direct correlation functions are used as additional input to the SCGLE representation for a size-asymmetric binary mixture, which was studied previously in Refs.[33, 48].

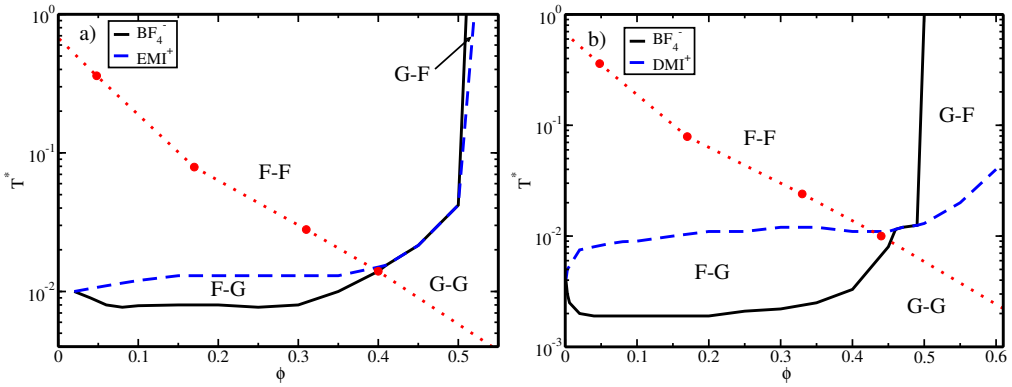

FIG. 2. Kinetic arrest diagrams as function of the total packing fraction ϕ_T and the reduced temperature T^* inspired by both C_nMIm systems, namely, (a) n=2 and (b) n=10. Four distinct regions are apparent, characterized by the mobility of the cation and anion species (with cation listed first): a completely fluid region (F–F), a completely arrested region (G–G), and two partially-arrested regimes (F–G and G–F). Within regions G–F, the hard-sphere interactions dominate leading to the dynamic arrest of the bigger particles due to caging. If the size difference between species is enough, small particles can diffuse through the holes left by the big particles (see [56] for additional details). On the other hand, in regions F–G the small particles become arrested due to high electrostatic repulsion between anions, leading to enough space for diffusion of the cations, a state known as winger glass (see [33]). Red lines shown in both figures represent an isobaric trajectory which mimics the cooling process performed in the simulated systems.

A numerical solution to the Ornstein–Zernike equation under the conditions outlined above may be computed for the non-trivial case of size asymmetry. The consequent structure factors $S_{ij}(k)$ are introduced into the SCGLE equilibrium equations in Fourier space to obtain the arrest factor γ_i which characterizes the mobility of each ionic species.

$$\frac{1}{\gamma_i} = \frac{1}{3(2\pi)^3}\int d^3k k^2 \Big\{\lambda\big[\lambda + k^2\gamma\big]^{-1}\Big\}_{ii}\Big\{c\sqrt{n}\lambda S\big[\lambda S + k^2\gamma\big]^{-1}\sqrt{n}h\Big\}_{ii}$$

Here, $\lambda(k)$ is a diagonal matrix with elements $\lambda_{ij} \equiv \delta_{ij}[1+(k/k_c^i)^2]^{(-1)}.$, and $k_c^i = 2\pi(1.305)/\sigma_i$ is an interpolation parameter whose value has been chosen to reproduce previous results [46]. The $c_{ij}(k)$ and $h_{ij}(k)$ are the correlation functions in Eq. 1 and the matrix n is defined by $(\sqrt{n})_{ij} \equiv \delta_{ij}\sqrt{n_i}$ where n_i is the number density of species i. The complete formulation of Eq. 2 has been reported in detail by Juarez-Maldonado and Medina-Noyola [53]. What is most relevant here is its physical meaning.

The parameter γ_i has a unique value for each pair of thermodynamic properties in our system, specifically $\phi_{\rm T}$ and T^*, where ϕ_T is the total volume fraction of our binary hard sphere mixture ($\phi_T = \pi(n_p\sigma_p^3 + n_m\sigma_m^3)/6$) and $T^* = k_BT\sigma_{ij}\varepsilon_0/e^2$ is the reduced temperature. Values of $\gamma_i \to \infty$ correspond to ergodic fluid states, while finite values of $\gamma_i < 1.0$ define glassy arrested states. By fixing the value of $\phi_{\rm T}$ (which defines an isochore) and computing γ_i values for one species within a range of temperatures, it is possible to map the change in values and delimit regions in the phase space which exhibit kinetic arrest of one or both species. The results are shown in Fig. 2 where four distinct regions have been found for changes in values of γ_i for the cation and anion species. In each "phase", the kinetic state (fluid F or glass G) of the cation is listed first and that of the anion is listed second. The lower region corresponds to finite small values of γ_i in both species, and is a completely arrested phase. At higher temperatures, adhesive interactions between opposite charges are suppressed, so that in systems which have low enough volume fraction to avoid jamming both species have fluid-like mobility. More interesting is the regions at top right (high volume fraction, high temperature) where only one of the ionic species is arrested. The partially-arrested F-G and G-F regions will be the focus of our subsequent analysis.

In order to collect further insights into the phase transition phenomena being observed, we will select several points in the arrest diagram, following the isobaric trajectories ($p = 1$ atm) shown as the red dashed lines in Fig. 2, and we will calculate the diffusion coefficient of the two ionic species at each region using the dynamic version of the SCGLE theory. This framework has been extensively explored and specifics of its implementation and analysis are presented in detail elsewhere [48, 57–59]. The dynamic version of the SCGLE framework requires the same input as before, which is the structure factor for each ionic species, and

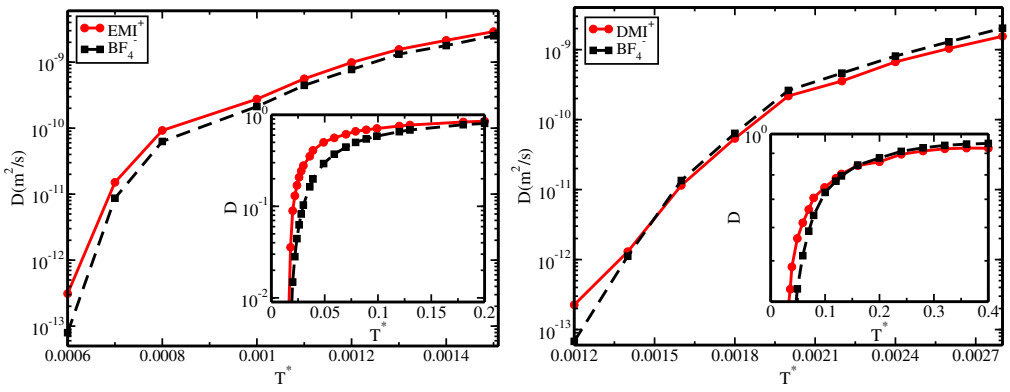

FIG. 3. Diffusion coefficient versus reduced temperatures for the systems studied. Main panels show the obtained results using all-atom simulations. The insets contain the theoretical calculations. At the left we present the results for the EMIM-BF4 system and the corresponding theoretical results for a primitive model with a size asymmetry of $\xi = \sigma_p/\sigma_m = 0.69nm/0.2nm$. At the right the results for DMIM-BF4 and a primitive model with $\xi = 1.46nm/0.2nm$. Notice the crossover for the system with the larger asymmetry which is observed in both simulation and theory. We observe a qualitative agreement among simulation and theory.

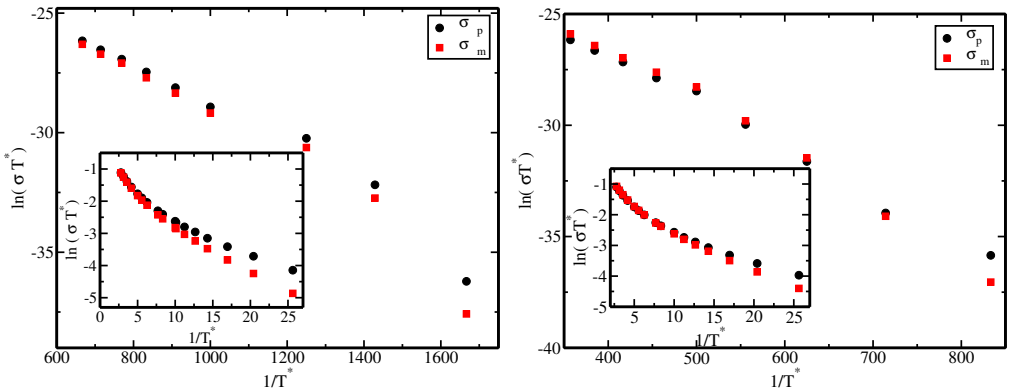

FIG. 4. Qualitative comparison of the overall conductivity of the studied systems. The main panel contains the results for the simulated systems and the insets the theoretical calculations. At the left we show the results for the system with the smallest asymmetry and at the right the system with the larger asymmetry. Both simulation and theory describe the same qualitative behavior.

unique values of total volume fraction ϕ_T and reduced temperature T^*. Several dynamic quantities are obtained in the solution of the coupled SCGLE equations, one of which is the diffusion coefficient. The results of our calculations are shown in Fig. 3, where insets exhibit theoretical predictions and main figures present all-atom simulation results. We can

observe that both theory and simulation present the same trends, probing the reliability of the SCGLE theoretical predictions.

We can utilize our solutions to extract the electrical conductivity, $\sigma \approx D_L$ for each ionic species, where D_L is the long-time diffusion coefficient [60]. In Fig. 4, the logarithm of the conductivity times the reduced temperature as a function of the inverse of the reduced temperature is calculated for both species at the involved asymmetries, namely a) $\xi = 3.5$, and b) $\xi = 7.2$. From Fig. 4 we observe a qualitative agreement between theory and simulation, despite the complexity of the ionic liquids considered to probe the theoretical predictions, we observe the same trends in both results. This is remarkable since it shows that the simpler model of ionic liquids is still useful in order to explore novel phases or behaviors in complex ionic liquids. Importantly, it also permits us to explore other regions and protocols where conductivity could be enhanced. In addition, our results are in complete agreement with previously reported studies, [33, 47, 61], where partially-arrested regions emerge with the larger ionic species diffusing among the smaller ionic species. This is a counter-intuitive behavior, though this phenomenon can be explained by a less efficient charge screening of the larger ions from the smaller ones, due to volume effects, and thus the small ion–small ion electrostatic interaction is effectively stronger than the opposite charged interaction, to the point where it promotes the formation of a glass phase of smaller ions while large ions remain fluid. Thus, the electronic conductivity is possible due to the anomalous diffusion of only one species of larger ions in a glassy state of smaller ions.

For practical applications, however, we are interested in the explicit case where the cations become arrested but anions remain fluid. Since charges may be exchanged in our model without changing any of the thermodynamic and dynamic behavior, this configuration is a representative state for ionic liquid crystals such as those comprising the polymers in Ref. [62] with small lithium cations and bulky TFSI-derived anions. Our results suggest bulky cations can be immobilized by steric hindrance (or other molecular interactions) leaving the smaller species free to move through the electrolyte. This presents an intriguing design strategy for single-ion conductors where the salt species is designed to maximize the glassiness of the macro-ionic species at concentrations and temperatures where the micro-ion remains mobile.

V. CONCLUSION

In this work, a theoretical binary mixture of charged hard spheres is analyzed in the framework of the Self Consistent Generalized Langevin Equation Theory (SCGLE). In the equilibrium version of the SCGLE, the γ_i parameter is used to determine limit lines where arrest states for each i species exist. A point in this phase space is characterized by a unique coordinate pair of ϕ_T and T^* parameters, the total volume fraction and the reduced temperature, respectively. This enables determination of a kinetic arrest diagram for a given size asymmetry of charged particles via the dynamic SCGLE theory. Results here are in agreement with prior equilibrium results, but are able to elucidate partially-arrest regions that may be exploited for their novel charge transport behavior. These regions occur for considerable size asymmetries between cation and anion (such as the 3.5:1 and 7.3:1 ratios explored here), and are anticipated to be relevant for systems such as ionic liquid crystals and polymerized ionic liquids, where interstitial conductive domains arise between arrested cations. Let us remark the power of such a simple model, based on a spherical approximation for ions and an analytic solution for structural properties, which offers an overall scenario consistent with all-atom MD simulation. Of course, refined models, which take into account the cation form and other effects, need to be implemented in order to obtain better comparison between theory and MD simulation. However, the application of simple models which capture the essential features represent a good first approach to complex problems. The main problem with the simple model used in this study is the incorrect mapping in the temperature values. Refinement of the structural solutions will be explored in the near future, since it could benefit the correct mapping over real temperature values, implying a possible quantitative comparison with simulation or experimental data. Even with the theoretical limitations, these results demonstrate new and significant behaviors relevant for developing energy storage technologies and offer predictions which may be realized by engineering new molecular structures and materials.

ACKNOWLEDGMENTS

PERG appreciates the assistance of J. Limón Castillo and acknowledge LANIMFE for the infrastructure provided during this project. JCAS, MFA and PERG acknowledge the

financial support of CONAHCyT through grants: programa de becas de posgrado, IxM No. 1631 and 7119. As well the grant CF-2023-I-1013. JKW acknowledges support from the NSF CAREER award, DMR-1751988. ECCM and JKW additionally acknowledge travel support from the University of Notre Dame through an International Collaboration Grant.

---

[1] N. V. Plechkova and K. R. Seddon, Chem. Soc. Rev. **37**, 123 (2008).

[2] A. P. Abbott, D. Boothby, G. Capper, D. L. Davies, and R. K. Rasheed, Journal of the American Chemical Society **126**, 9142 (2004).

[3] H. Ohno, Bulletin of the Chemical Society of Japan **79**, 1665 (2006).

[4] A. Lewandowski and A. Świderska Mocek, Journal of Power Sources **194**, 601 (2009).

[5] D. Zhao, M. Wu, Y. Kou, and E. Min, Catalysis Today **74**, 157 (2002), environmentally Benign Petrochemical Catalytic Chemistry and Reaction Engineering 2002.

[6] H. Olivier-Bourbigou, L. Magna, and D. Morvan, Applied Catalysis A: General **373**, 1 (2010).

[7] J. Lu, F. Yan, and J. Texter, Progress in Polymer Science **34**, 431 (2009).

[8] J. Guo, Z. D. Tucker, Y. Wang, B. L. Ashfeld, and T. Luo, Nature Communications **12**, 437 (2021).

[9] K. Dong and S. Zhang, Chemistry – A European Journal **18**, 2748 (2012).

[10] J. Tong, Y. Guo, F. Huo, X. Xie, H. He, N. von Solms, X. Liang, and S. Zhang, Industrial & Engineering Chemistry Research **57**, 15206 (2018).

[11] W. Cao, Y. Wang, and G. Saielli, The Journal of Physical Chemistry B **122**, 229 (2018).

[12] M. J. Quevillon and J. K. Whitmer, Materials **11** (2018), 10.3390/ma11010064.

[13] M. G. Del Pópolo and G. A. Voth, The Journal of Physical Chemistry B **108**, 1744 (2004).

[14] K. Binnemans, Chemical Reviews **105**, 4148 (2005).

[15] A. Rivera, A. Brodin, A. Pugachev, and E. Rössler, The Journal of chemical physics **126** (2007).

[16] J. Sangoro, C. Iacob, A. Serghei, C. Friedrich, and F. Kremer, Physical Chemistry Chemical Physics **11**, 913 (2009).

[17] J. R. Sangoro and F. Kremer, Accounts of chemical research **45**, 525 (2012).

[18] P. Sippel, P. Lunkenheimer, S. Krohns, E. Thoms, and A. Loidl, Scientific reports **5**, 13922 (2015).

[19] T. Pal and M. Vogel, ChemPhysChem **18**, 2233 (2017).

[20] A. Weyman, M. Bier, C. Holm, and J. Smiatek, The journal of chemical physics **148** (2018).

[21] M. Becher, E. Steinrücken, and M. Vogel, The Journal of chemical physics **151** (2019).

[22] S. Tian, Y. Luo, Z. Zhao, N. Deng, and G. Ren, Journal of Molecular Modeling **26**, 1 (2020).

[23] E. Steinrücken, M. Becher, and M. Vogel, The Journal of Chemical Physics **153** (2020).

[24] J. F. Rudzinski, S. Kloth, S. Wörner, T. Pal, K. Kremer, T. Bereau, and M. Vogel, Journal of Physics: Condensed Matter **33**, 224001 (2021).

[25] S. Kloth, M. P. Bernhardt, N. F. van der Vegt, and M. Vogel, Journal of Physics: Condensed Matter **33**, 204002 (2021).

[26] C. Tang and Y. Wang, Communications in Theoretical Physics **74**, 097601 (2022).

[27] E. Axinte, Materials and Design **35**, 518 (2012), new Rubber Materials, Test Methods and Processes.

[28] D. B. Miracle, Nature Materials **3**, 697 (2004).

[29] M. J. Abraham, T. Murtola, R. Schulz, S. Páll, J. C. Smith, B. Hess, and E. Lindahl, SoftwareX **1**, 19 (2015).

[30] S. Páll, M. J. Abraham, C. Kutzner, B. Hess, and E. Lindahl, in *Solving Software Challenges for Exascale: International Conference on Exascale Applications and Software, EASC 2014, Stockholm, Sweden, April 2-3, 2014, Revised Selected Papers 2* (Springer, 2015) pp. 3–27.

[31] W. D. Cornell, P. Cieplak, C. I. Bayly, I. R. Gould, K. M. Merz, D. M. Ferguson, D. C. Spellmeyer, T. Fox, J. W. Caldwell, and P. A. Kollman, Journal of the American Chemical Society **118**, 2309 (1996).

[32] Y. Wang and G. A. Voth, Journal of the American Chemical Society **127**, 12192 (2005).

[33] P. E. Ramírez-González, L. E. Sanchéz-Díaz, M. Medina-Noyola, and Y. Wang, The Journal of Chemical Physics **145**, 191101 (2016).

[34] M. P. Allen and D. J. Tildesley, *Computer simulation of liquids* (Oxford university press, 2017).

[35] D. Frenkel and B. Smit, *Understanding molecular simulation: from algorithms to applications* (Elsevier, 2023).

[36] U. Essmann, L. Perera, M. L. Berkowitz, T. Darden, H. Lee, and L. G. Pedersen, The Journal of chemical physics **103**, 8577 (1995).

[37] P. E. Ramirez-Gonzalez, G. Ren, G. Saielli, and Y. Wang, The Journal of Physical Chemistry B **120**, 5678 (2016).

[38] L. S. Ornstein and F. Zernike, in *Proc. Acad. Sci. Amsterdam*, Vol. 17 (1914) p. 793.

[39] E. Waisman and J. L. Lebowitz, The Journal of Chemical Physics **56**, 3086 (1972).

[40] E. Waisman and J. L. Lebowitz, The Journal of Chemical Physics **56**, 3093 (1972).

[41] J.-P. Simonin, L. Blum, and P. Turq, The Journal of Physical Chemistry **100**, 7704 (1996).

[42] H. Weingärtner, Angewandte Chemie International Edition **47**, 654 (2008).

[43] G. Stell and S. F. Sun, The Journal of Chemical Physics **63**, 5333 (1975).

[44] O. Bernard, J. Torres-Arenas, and J.-P. Simonin, The Journal of Chemical Physics **140**, 034502 (2014).

[45] J. Lira-Escobedo, P. Mendoza-Méndez, M. Medina-Noyola, G. B. McKenna, and P. E. Ramírez-González, The Journal of Chemical Physics **155**, 14503 (2021).

[46] L. E. Sánchez-Díaz, A. Vizcarra-Rendón, and R. Juárez-Maldonado, Physical Review Letters **103**, 35701 (2009).

[47] N. Benitez-Camacho, J. M. Olais-Govea, L. López-Flores, and H. Ruiz-Estrada, The Journal of Chemical Physics **159** (2023).

[48] M. E. Farias-Anguiano, L. E. Sánchez-Díaz, E. C. Cortés-Morales, and P. E. Ramírez-González, Physics of Fluids **34** (2022).

[49] S.-W. Ryu, P. E. Trapa, S. C. Olugebefola, J. A. Gonzalez-Leon, D. R. Sadoway, and A. M. Mayes, Journal of The Electrochemical Society **152**, A158 (2005).

[50] L. Porcarelli, A. S. Shaplov, F. Bella, J. R. Nair, D. Mecerreyes, and C. Gerbaldi, ACS Energy Letters **1**, 678 (2016).

[51] L. Elizondo-Aguilera, P. Zubieta Rico, H. Ruiz-Estrada, and O. Alarcón-Waess, Physical Review E **90**, 052301 (2014).

[52] R. Peredo-Ortiz, P. F. Z. Rico, E. C. Cortés-Morales, G. G. Pérez-Ángel, T. Voigtmann, M. Medina-Noyola, and L. F. Elizondo-Aguilera, Journal of Physics: Condensed Matter **34**, 084003 (2021).

[53] R. Juárez-Maldonado and M. Medina-Noyola, Physical Review E **77**, 51503 (2008).

[54] K. Hiroike, Molecular Physics **33**, 1195 (1977).

[55] L. Blum, Molecular Physics **30**, 1529 (1975).

[56] R. Juárez-Maldonado and M. Medina-Noyola, Physical Review Letters **101**, 267801 (2008).

[57] L. Yeomans-Reyna and M. Medina-Noyola, Physical Review E **64**, 66114 (2001).

[58] M. A. Chávez-Rojo and M. Medina-Noyola, Physical Review E **72**, 31107 (2005).

[59] L. Yeomans-Reyna, M. A. Chávez-Rojo, P. E. Ramírez-González, R. Juárez-Maldonado, M. Chávez-Páez, and M. Medina-Noyola, Physical Review E **76**, 41504 (2007).

[60] B. Roling, C. Martiny, and S. Brückner, Physical Review B **63**, 214203 (2001).

[61] E. Sanz, M. E. Leunissen, A. Fortini, A. van Blaaderen, and M. Dijkstra, The Journal of Physical Chemistry B **112**, 10861 (2008).

[62] L. C. Merrill, X. C. Chen, Y. Zhang, H. O. Ford, K. Lou, Y. Zhang, G. Yang, Y. Wang, Y. Wang, J. L. Schaefer, and N. J. Dudney, ACS Applied Energy Materials **3**, 8871 (2020).